

Effect of intersubband scattering on weak localization in 2D systems

N.S. Averkiev,¹ L.E. Golub,^{1,2} S.A. Tarasenko*,¹ and M. Willander²

¹*A.F. Ioffe Physico-Technical Institute, Russian Academy of Sciences, 194021 St. Petersburg,
Russia*

²*Physical Electronics and Photonics, Department of Physics, Chalmers University of Technology
and Göteborg University, S-412 96, Göteborg, Sweden*

(October 31, 2018)

Abstract

The theory of weak localization is generalized for multilevel 2D systems taking into account intersubband scattering. It is shown that weak intersubband scattering which is negligible in a classical transport, affects strongly the weak-localization correction to conductivity. The anomalous magnetoresistance is calculated in the whole range of classically low magnetic fields. This correction to conductivity is shown to depend strongly on the ratios of occupied level concentrations. It is demonstrated that at relatively low population of the excited subband, it is necessary to use the present theory because the high-field limit asymptotics is shown to be achieved only in classical magnetic fields.

PACS: 73.20.Fz, 73.63.Hs, 73.21.-b

Typeset using REVTeX

*E-mail: tarasenko@coherent.ioffe.rssi.ru

I. INTRODUCTION

Weak localization phenomenon is an interference of waves propagating along the same paths in opposite directions. Phase and spin relaxation processes or magnetic field destroy the interference and therefore can make observable the weak localization effect. The most remarkable manifestation of the phenomenon is the anomalous behavior of resistance in classically weak magnetic fields. This effect takes place when the magnetic length, l_B , is simultaneously comparable to characteristic kinetic lengths.

In very low magnetic fields, when the mean free path, l , is much less than l_B the coherence is lost at long trajectories. This is so-called *diffusion* regime of weak localization, and the corresponding characteristic size is the dephasing length, l^φ . In higher fields, when $l_B \sim l$, the short trajectories passing through several scatterers contribute to weak localization. This regime is called *non-diffusion*.

The anomalous magnetoresistance was widely investigated both theoretically and experimentally in bulk semiconductors and metals, thin films and ultra-quantum two-dimensional (2D) structures. A comparison of theory and experimental data allowed to determine the kinetic parameters as times and lengths of elastic relaxation and dephasing.¹

Recently magnetotransport has been investigated in more complicated systems which are between 3D and 2D ones. The weak localization experiments were performed on 2D multivalley semiconductors², quantum wells with two or several occupied levels of size quantization,³⁻⁵ doped δ -layers,⁶ and on tunnel-coupled quantum wells.⁷ In these quasi-two-dimensional (quasi-2D) systems, the intersubband scattering takes place. It leads to effective averaging of the kinetic parameters corresponding to different levels, and therefore affects a magnitude and behavior of magnetotransport characteristics.⁸ Quasi-2D systems are very attractive objects for study of weak localization because even rare intersubband transitions affect it strongly. Usually the scattering time for transition between α^{th} and β^{th} subbands, $\tau_{\alpha\beta}$ ($\alpha \neq \beta$), exceeds enough the total momentum relaxation times in subbands, τ_α , therefore an influence of intersubband scattering on classical magnetotransport

is insignificant. In opposite, the dependence of weak-localization correction to conductivity on magnetic field, $\Delta\sigma(B)$, is determined by the dephasing time τ_α^φ exceeding τ_α . Therefore at $\tau_{\alpha\beta}$ long with respect to τ_α but comparable to τ_α^φ , intersubband scattering affects weak-localization correction strongly.

To describe the experimental data, one needs the weak-localization theory taking into account the intersubband scattering for the whole range of classically low magnetic fields. However the theory was developed only for simple systems with one populated level.⁹ The intersubband scattering was considered only in the diffusion regime.^{10–14}

The aim of the present paper is to develop the theory of weak localization in quasi-2D systems for the whole range of classically low magnetic fields. It is the theory that is necessary for quantitative determining of kinetic parameters of structures by comparison with experimental data.

The paper is organized as follows. In Section II we derive the expressions for the weak-localization correction to the conductivity. Section III is devoted to the detailed analysis of two occupied subband system. The main results are given briefly in Conclusion.

II. THEORY

Since intersubband scattering is accompanied by large transfer of the momentum, it is caused mainly by the short-range part of the potential. Therefore to attract attention to effect of the intersubband transitions, the scattering is assumed to be from short-range potential, e.g. impurities. The main weak-localization corrections to the conductivity appear in the first order in the parameter $(k_F l)^{-1}$, where k_F is the Fermi wavevector. The corresponding diagrams for the corrections are presented in Fig. 1. The dashed lines conform to the correlation function of the total potential $V(\boldsymbol{\rho}, z)$, where $\boldsymbol{\rho} = (x, y)$ are the coordinates in the 2D plane and z is the perpendicular direction. Providing δ -scattering, this correlator has the form

$$\langle V(\boldsymbol{\rho}, z)V(\boldsymbol{\rho}', z') \rangle = W\delta(\boldsymbol{\rho} - \boldsymbol{\rho}')\delta(z - z')f(z). \quad (1)$$

Here the averaging is performed over the impurity positions, $f(z)$ is the function of scatterer distribution, and W is the factor dependent on intensity and concentration of scatterers. The solid lines in the diagrams describe the Green functions of the quasi-2D electron gas in an external magnetic field. We assume the condition of a “good conductor” to be fulfilled for all subbands

$$\mu_\alpha \tau_\alpha / \hbar \gg 1, \quad (2)$$

and the energy distances between subbands are large

$$|\mu_\alpha - \mu_\beta| \gg \hbar / \tau_\alpha. \quad (3)$$

Here μ_α is the chemical potential counted from the bottom of the α^{th} subband, and τ_α is the momentum relaxation time of carriers in the subband,

$$1/\tau_\alpha = \sum_\beta 1/\tau_{\alpha\beta}, \quad (4)$$

where $\tau_{\alpha\beta} = \tau_{\beta\alpha}$ is the scattering time between the α^{th} and β^{th} subbands, and summation is performed over all occupied levels of size quantization. Since $\tau_{\alpha\beta}$ arises due to scattering from impurities, it is defined by the following relation

$$1/\tau_{\alpha\beta} = \frac{2\pi}{\hbar} N_F W \int f(z) u_\alpha^2(z) u_\beta^2(z) dz, \quad (5)$$

where $N_F = m/(2\pi\hbar^2)$ is the density of states at Fermi level with a fixed spin, and m is the electron effective mass in the 2D plane.

The advanced and retarded Green functions are diagonal in subband indices under conditions (2), (3)^{15,16}

$$G_\alpha^{A,R}(\boldsymbol{\rho}, z, \boldsymbol{\rho}', z') = \sum_\alpha G_\alpha^{A,R}(\boldsymbol{\rho}, \boldsymbol{\rho}') u_\alpha(z) u_\alpha(z'),$$

$$G_\alpha^{A,R}(\boldsymbol{\rho}, \boldsymbol{\rho}') = \sum_{Nk_y} \frac{\psi_{Nk_y}(\boldsymbol{\rho}) \psi_{Nk_y}^*(\boldsymbol{\rho}')}{\mu_\alpha - \hbar\omega_c(N + 1/2) \pm i\hbar/2\tau_\alpha \pm i\hbar/2\tau_\alpha^\varphi}. \quad (6)$$

Here $\psi_{Nk_y}(\boldsymbol{\rho}) u_\alpha(z)$ is the electron wave function in the heterostructure in the Landau gauge with the vector potential directed along the y axis, N and k_y are the number of the Landau level and the value of the in-plane wavevector, ω_c is the cyclotron frequency, and the dephasing time τ_α^φ ($\tau_\alpha^\varphi \gg \tau_\alpha$) describes inelastic scattering.

In a classically weak magnetic field, when $\omega_c\tau_\alpha \ll 1$, the field dependence appears only in the phase of the Green functions, similarly to the case of one subband occupation:

$$G_\alpha^{A,R}(\boldsymbol{\rho}, \boldsymbol{\rho}') = \exp[i\Phi(\boldsymbol{\rho}, \boldsymbol{\rho}')] G_\alpha^{(0)A,R}(\boldsymbol{\rho} - \boldsymbol{\rho}'). \quad (7)$$

The phase factor is given by

$$\Phi(\boldsymbol{\rho}, \boldsymbol{\rho}') = \frac{(y' - y)(x' + x)}{2l_B^2}, \quad (8)$$

and $G_\alpha^{(0)A,R}$ are the Green functions in zero magnetic field

$$G_\alpha^{(0)A,R}(\boldsymbol{\rho} - \boldsymbol{\rho}') = -2N_F K_0 \left[\pm i k_\alpha |\boldsymbol{\rho} - \boldsymbol{\rho}'| + \frac{|\boldsymbol{\rho} - \boldsymbol{\rho}'|}{2l_\alpha} \left(1 + \frac{l_\alpha}{l_\alpha^\varphi} \right) \right], \quad (9)$$

where $l_B = \sqrt{\hbar c/|e|B}$ is the magnetic length, with $e < 0$ and B being the electron charge and magnetic field, K_0 is the McDonald function, k_α , $l_\alpha = \hbar k_\alpha \tau_\alpha / m$ and $l_\alpha^\varphi = \hbar k_\alpha \tau_\alpha^\varphi / m$ are the Fermi wavevector, the mean free path and the dephasing length in the α^{th} subband, respectively.

Figs. 1a-d show all types of diagrams contributing to the anomalous magnetoconductivity. The similar diagrams with two scattering lines are depicted in Fig. 1e.

The latter are special. In the papers^{17,18} they were calculated incorrect way and therefore a non-physical divergence was obtained. It was noted in Ref. 9 that two-impurity line diagrams correspond to non-self-crossing trajectories which have zero magnetic flux passing through them and, hence, a field does not change this correction to the conductivity, $\Delta\sigma_2$. In Ref. 19 the contribution was investigated in more detail. It was shown formally that $\Delta\sigma_2$ is independent of magnetic field and its value has an order of e^2/\hbar . However the calculation of $\Delta\sigma_2$ was not performed. It was claimed in Ref. 20 that $\Delta\sigma_2 = 0$, however the proof of this statement was absent.

Thus, $\Delta\sigma_2$ i) has never been calculated and ii) it was claimed without proof that $\Delta\sigma_2 = 0$. Below we calculate this contribution and show that it is not equal to zero.

A. Contribution from the diagrams with two scattering lines

The expression for the conductivity correction from the diagrams with two scattering lines (Fig. 1e) has the form

$$\Delta\sigma_2 = \frac{\hbar}{2\pi} \sum_{\alpha\beta\gamma\delta} W_{\alpha\beta\gamma\delta}^2 \int \int d\rho_1 d\rho_2 \mathbf{J}_\alpha^{RA}(\rho_2, \rho_1) \cdot \left[\mathbf{J}_\beta^{AR}(\rho_2, \rho_1) G_\gamma^A(\rho_1, \rho_2) G_\delta^R(\rho_1, \rho_2) + \mathbf{J}_\beta^{AR}(\rho_1, \rho_2) G_\gamma^A(\rho_1, \rho_2) G_\delta^A(\rho_2, \rho_1) + \mathbf{J}_\beta^{AR}(\rho_1, \rho_2) G_\gamma^R(\rho_1, \rho_2) G_\delta^R(\rho_2, \rho_1) \right]. \quad (10)$$

Here the spin degeneracy has been taken into account,

$$W_{\alpha\beta\gamma\delta} = W \int f(z) u_\alpha(z) u_\beta(z) u_\gamma(z) u_\delta(z) dz, \quad (11)$$

and the current vertex is defined as

$$\mathbf{J}_\alpha^{RA}(\rho, \rho') = \int d\rho_1 G_\alpha^R(\rho, \rho_1) \hat{\mathbf{J}}(\rho_1) G_\alpha^A(\rho_1, \rho'), \quad (12)$$

where $\hat{\mathbf{J}}$ is the electric current operator. In classically low magnetic fields, the vertices have the form

$$\mathbf{J}_\alpha^{RA}(\rho, \rho') = \mathbf{J}_\alpha^{AR}(\rho, \rho') = \exp[i\Phi(\rho, \rho')] \mathbf{J}_\alpha^{(0)}(\rho - \rho'), \quad (13)$$

where $\mathbf{J}^{(0)}$ is the current vertex in zero magnetic field

$$\mathbf{J}_\alpha^{(0)}(\rho - \rho') = \frac{e\tau_\alpha}{m} \nabla_\rho \left[G_\alpha^{(0)R}(\rho - \rho') - G_\alpha^{(0)A}(\rho - \rho') \right]. \quad (14)$$

One can see, the conductivity correction $\Delta\sigma_2$ is independent of magnetic field, because the current vertices in (10), $\mathbf{J}_\alpha(\rho_2, \rho_1)$, contain the phase factor which is complex conjugated to that contained in $G_\beta(\rho_1, \rho_2)$.

Taking into account (7), (9), (13), (14) and providing the limits $k_\alpha l_\alpha \rightarrow \infty$, $l_\alpha/l_\alpha^\varphi \rightarrow \infty$, we obtain the contribution of the diagrams with two impurity lines

$$\begin{aligned} \Delta\sigma_2 = & -\frac{e^2}{\pi^4 \hbar} \sum_{\alpha\beta\gamma\delta} \left(\frac{2\pi}{\hbar} N_F W_{\alpha\beta\gamma\delta} \right)^2 \tau_\alpha \tau_\beta \\ & \times k_\alpha k_\beta \int_0^\infty d\rho \rho [K_1(ik_\alpha \rho) + K_1(-ik_\alpha \rho)] [K_1(ik_\beta \rho) + K_1(-ik_\beta \rho)] \\ & \times [K_0(ik_\gamma \rho) K_0(-ik_\delta \rho) - K_0(ik_\gamma \rho) K_0(ik_\delta \rho) - K_0(-ik_\gamma \rho) K_0(-ik_\delta \rho)]. \quad (15) \end{aligned}$$

The asymptotic expansions for K_0 and K_1 at large arguments have not to be used for calculation of $\Delta\sigma_2$, otherwise the integrand tends to infinity at $\rho \rightarrow 0$. It is the mistake that was done in Refs. 17,18.

Eq. (15) shows that the diagrams with two impurity lines give rise to non-zero contribution to the conductivity contrary to the notice in Ref. 20. For the case of one occupied subband, we obtain (see Appendix)

$$\Delta\sigma_2 = -\frac{e^2}{\pi^2\hbar} \ln 2. \quad (16)$$

B. Magnetoconductivity calculation

Now, we consider the weak-localization corrections which do contribute to the anomalous magnetoresistance. The corresponding diagrams are presented in Fig. 1a-d. One can show the terms c) and d) cancel out each other similarly to the case of one occupied subband. Thus the field-sensitive conductivity correction has the form

$$\Delta\sigma = \Delta\sigma^{(a)} + \Delta\sigma^{(b)}, \quad (17)$$

$$\Delta\sigma^{(a)} = \frac{\hbar}{2\pi} \sum_{\alpha} \int d\rho_1 d\rho_2 \mathbf{J}_{\alpha}^{RA}(\rho_2, \rho_1) \cdot \mathbf{J}_{\alpha}^{AR}(\rho_2, \rho_1) \mathcal{C}_{\alpha\alpha}^{(3)}(\rho_1, \rho_2), \quad (18)$$

$$\begin{aligned} \Delta\sigma^{(b)} = & \frac{\hbar}{\pi} \sum_{\alpha\beta} \int d\rho_1 d\rho_2 d\rho_3 \left[J_{x\alpha}^{RA}(\rho_3, \rho_1) J_{x\beta}^{AR}(\rho_1, \rho_2) \mathcal{C}_{\beta\alpha}^{(2)}(\rho_2, \rho_3) G_{\beta}^A(\rho_1, \rho_2) G_{\alpha}^A(\rho_3, \rho_1) \right. \\ & \left. + J_{x\alpha}^{RA}(\rho_1, \rho_2) J_{x\beta}^{AR}(\rho_3, \rho_1) \mathcal{C}_{\alpha\beta}^{(2)}(\rho_2, \rho_3) G_{\beta}^R(\rho_3, \rho_1) G_{\alpha}^R(\rho_1, \rho_2) \right] W_{\alpha\alpha\beta\beta}, \quad (19) \end{aligned}$$

where $J_{x\alpha}$ is the x -projection of the vector \mathbf{J}_{α} , and the Cooperons $\mathcal{C}^{(2)}$ and $\mathcal{C}^{(3)}$ are the sums of the fan internal parts of the corresponding diagrams starting with two and three lines, respectively. In general, these parts depend on four subband indices. However one can show the Cooperons are diagonal in the pairs of indices due to the relations (2), (3) similarly to the Green functions (see Eq. 6).

The Cooperons $\mathcal{C}^{(2)}$ and $\mathcal{C}^{(3)}$ can be found from the following systems of equations

$$\begin{aligned}
\mathcal{C}_{\alpha\beta}^{(2)}(\boldsymbol{\rho}, \boldsymbol{\rho}') &= \frac{2\pi N_F}{\hbar} \sum_{\gamma} W_{\alpha\alpha\gamma\gamma} W_{\gamma\gamma\beta\beta} \tau_{\gamma} P_{\gamma}(\boldsymbol{\rho}, \boldsymbol{\rho}') \\
&\quad + \frac{2\pi N_F}{\hbar} \sum_{\gamma} W_{\alpha\alpha\gamma\gamma} \tau_{\gamma} \int d\boldsymbol{\rho}_1 P_{\gamma}(\boldsymbol{\rho}, \boldsymbol{\rho}_1) \mathcal{C}_{\gamma\beta}^{(2)}(\boldsymbol{\rho}_1, \boldsymbol{\rho}'), \\
\mathcal{C}_{\alpha\beta}^{(3)}(\boldsymbol{\rho}, \boldsymbol{\rho}') &= \mathcal{C}_{\alpha\beta}^{(2)}(\boldsymbol{\rho}, \boldsymbol{\rho}') - \frac{2\pi N_F}{\hbar} \sum_{\gamma} W_{\alpha\alpha\gamma\gamma} W_{\gamma\gamma\beta\beta} \tau_{\gamma} P_{\gamma}(\boldsymbol{\rho}, \boldsymbol{\rho}'),
\end{aligned} \tag{20}$$

where

$$P_{\alpha}(\boldsymbol{\rho}, \boldsymbol{\rho}_1) = \frac{\hbar}{2\pi N_F \tau_{\alpha}} G_{\alpha}^A(\boldsymbol{\rho}, \boldsymbol{\rho}_1) G_{\alpha}^R(\boldsymbol{\rho}, \boldsymbol{\rho}_1). \tag{21}$$

In order to solve the systems (20), we expand the kernel of the integral operator, $P_{\alpha}(\boldsymbol{\rho}, \boldsymbol{\rho}_1)$, in series of the 2D wave functions of a particle with the mass m and the charge $2e$ under a perpendicular magnetic field in the Landau gauge, $\chi_{Nk_y}(\boldsymbol{\rho})$. In this basis, $P_{\alpha}(\boldsymbol{\rho}, \boldsymbol{\rho}_1)$ is diagonal:^{9,18}

$$P_{\alpha}(\boldsymbol{\rho}, \boldsymbol{\rho}_1) = \sum_{Nk_y} P_{\alpha}(N) \chi_{Nk_y}(\boldsymbol{\rho}) \chi_{Nk_y}^*(\boldsymbol{\rho}_1). \tag{22}$$

From Eqs. (20) it follows that $\mathcal{C}_{\alpha\beta}^{(2)}(\boldsymbol{\rho}, \boldsymbol{\rho}_1)$ and $\mathcal{C}_{\alpha\beta}^{(3)}(\boldsymbol{\rho}, \boldsymbol{\rho}_1)$ are also diagonal in this basis:

$$\mathcal{C}_{\alpha\beta}^{(2,3)}(\boldsymbol{\rho}, \boldsymbol{\rho}_1) = \frac{\hbar}{2\pi N_F} \sum_{Nk_y} \mathcal{C}_{\alpha\beta}^{(2,3)}(N) \chi_{Nk_y}(\boldsymbol{\rho}) \chi_{Nk_y}^*(\boldsymbol{\rho}_1). \tag{23}$$

The asymptotics for the Green functions and the current vertex at long distances, $|\boldsymbol{\rho} - \boldsymbol{\rho}'| k_{\alpha} \gg 1$, can be used for calculation of the diagrams with three or more dashed lines. The corresponding expressions are

$$G_{\alpha}^{(0)A,R}(\boldsymbol{\rho} - \boldsymbol{\rho}') \approx -N_F \sqrt{\frac{2\pi}{k_{\alpha} |\boldsymbol{\rho} - \boldsymbol{\rho}'|}} \exp \left[\mp i \frac{\pi}{4} \mp i k_{\alpha} |\boldsymbol{\rho} - \boldsymbol{\rho}'| - \frac{|\boldsymbol{\rho} - \boldsymbol{\rho}'|}{2l_{\alpha}} \left(1 + \frac{l_{\alpha}}{l_{\alpha}^{\varphi}} \right) \right], \tag{24}$$

$$\mathbf{J}_{\alpha}^{(0)}(\boldsymbol{\rho} - \boldsymbol{\rho}') \approx i \frac{e}{\hbar} l_{\alpha} \left[G_{\alpha}^{(0)R}(\boldsymbol{\rho} - \boldsymbol{\rho}') + G_{\alpha}^{(0)A}(\boldsymbol{\rho} - \boldsymbol{\rho}') \right] \frac{\boldsymbol{\rho} - \boldsymbol{\rho}'}{|\boldsymbol{\rho} - \boldsymbol{\rho}'|}. \tag{25}$$

Thus, the coefficients for the expansion of the kernel are given by

$$P_{\alpha}(N) = \frac{l_B}{l_{\alpha}} \int_0^{\infty} dx \exp \left[-x \frac{l_B}{l_{\alpha}} \left(1 + \frac{l_{\alpha}}{l_{\alpha}^{\varphi}} \right) - \frac{x^2}{2} \right] L_N(x^2), \tag{26}$$

where L_N are the Laguerre polynomials. The values $\mathcal{C}^{(2)}(N)$ and $\mathcal{C}^{(3)}(N)$ are defined by the following systems of linear equations

$$\begin{aligned} \sum_{\gamma} \left(\delta_{\alpha\gamma} - \frac{\tau_{\gamma}}{\tau_{\alpha\gamma}} P_{\gamma}(N) \right) \mathcal{C}_{\gamma\beta}^{(2)}(N) &= \sum_{\gamma} \frac{\tau_{\gamma}}{\tau_{\alpha\gamma}\tau_{\gamma\beta}} P_{\gamma}(N), \\ \mathcal{C}_{\alpha\beta}^{(3)}(N) &= \mathcal{C}_{\alpha\beta}^{(2)}(N) - \sum_{\gamma} \frac{\tau_{\gamma}}{\tau_{\alpha\gamma}\tau_{\gamma\beta}} P_{\gamma}(N). \end{aligned} \quad (27)$$

Neglecting the rapidly oscillating terms $G^R G^R$ and $G^A G^A$ and taking into account the expansions (22), (23), we obtain

$$\Delta\sigma^{(a)} = -\frac{e^2}{\pi^2\hbar} \sum_{\alpha} \frac{l_{\alpha}^2}{l_B^2} \tau_{\alpha} \sum_{N=0}^{\infty} P_{\alpha}(N) \mathcal{C}_{\alpha\alpha}^{(3)}(N). \quad (28)$$

Expanding the expression $P_{\alpha}(\boldsymbol{\rho}, \boldsymbol{\rho}') \frac{\boldsymbol{\rho} - \boldsymbol{\rho}'}{|\boldsymbol{\rho} - \boldsymbol{\rho}'|}$ in series of the functions $\chi_{Nk_y}(\boldsymbol{\rho})$, one can also find

$$\Delta\sigma^{(b)} = \frac{e^2}{\pi^2\hbar} \sum_{\alpha\beta} \frac{l_{\alpha}l_{\beta}}{l_B^2} \frac{\tau_{\alpha}\tau_{\beta}}{\tau_{\alpha\beta}} \sum_{N=0}^{\infty} Q_{\alpha}(N)Q_{\beta}(N) \frac{1}{2} \left[\mathcal{C}_{\alpha\beta}^{(2)}(N) + \mathcal{C}_{\beta\alpha}^{(2)}(N+1) \right], \quad (29)$$

where

$$Q_{\alpha}(N) = \frac{l_B}{l_{\alpha}} \frac{1}{\sqrt{N+1}} \int_0^{\infty} dx x \exp \left[-x \frac{l_B}{l_{\alpha}} \left(1 + \frac{l_{\alpha}}{l_{\alpha}^{\varphi}} \right) - \frac{x^2}{2} \right] L_N^1(x^2). \quad (30)$$

with L_N^1 being the associated Laguerre polynomials.

Eqs. (28,29) describe the weak-localization correction to conductivity, $\Delta\sigma$, in the whole range of classically-weak fields, $\omega_c\tau \ll 1$, when l_B may be both larger and smaller than l_{α} . Now we consider the limiting cases.

In the zero-field limit, the large number of terms, up to $N \sim (l_B/l_{\alpha})^2$, is essential in the sums (28,29). Therefore to provide the calculation of $\Delta\sigma(0)$, the summation over N should be replaced by integration with the following zero-field asymptotics

$$P_{\alpha}(N) \approx \frac{1}{\sqrt{(1 + l_{\alpha}/l_{\alpha}^{\varphi})^2 + 4N(l_{\alpha}/l_B)^2}}, \quad Q_{\alpha}(N) \approx \frac{1 - (1 + l_{\alpha}/l_{\alpha}^{\varphi})P_{\alpha}(N)}{2\sqrt{N}l_{\alpha}/l_B}.$$

In low fields,

$$l_B \sim \sqrt{l_{\alpha}l_{\alpha}^{\varphi}} \gg l_{\alpha}, \quad (31)$$

the so-called diffusion approximation is valid. The interference is destroyed at long trajectories, where particles experience many scattering events and, hence, their motion is a

diffusion. In the frame of the approach, one can calculate the difference between quantum corrections in finite and zero fields $\Delta\sigma(B) - \Delta\sigma(0)$. To obtain the expression, the Cooperons determined from the system (27) should be sought in the form of diffusion poles.¹³ The difference $\Delta\sigma(B) - \Delta\sigma(0)$ due to the diagrams b) in Fig. 1 are small in fields (31), and therefore the correction behavior is defined by the low-field asymptotics of $\Delta\sigma^{(a)}$ only. The value of the conductivity correction in zero field itself, $\Delta\sigma(0)$, calculated with the diffusion approach is correct at $\ln(\tau_\alpha^\varphi/\tau_\alpha) \gg 1$ that is not realized practically.

In the particular case of two occupied subband system, the diffusion approximation yields the following magnetoconductivity correction

$$\Delta\sigma(B) - \Delta\sigma(0) = \frac{e^2}{2\pi^2\hbar} \left[f_2 \left(\frac{\tilde{l}_1^2}{l_B^2} \right) + f_2 \left(\frac{\tilde{l}_2^2}{l_B^2} \right) \right], \quad (32)$$

where $f_2(x) = \ln x + \psi(1/2 + 1/x)$, and $\psi(y)$ is the digamma-function. The lengths $\tilde{l}_{1,2}$ are given by^{12,13}

$$\tilde{l}_{1,2}^2 = \frac{4l_1l_2}{\frac{l_2}{l_1} \frac{\tau_1}{t_1} + \frac{l_1}{l_2} \frac{\tau_2}{t_2} \pm \sqrt{\left(\frac{l_2}{l_1} \frac{\tau_1}{t_1} - \frac{l_1}{l_2} \frac{\tau_2}{t_2} \right)^2 + 4 \frac{\tau_1\tau_2}{\tau_{12}^2}}},$$

where the corresponding times are

$$\frac{1}{t_{1,2}} = \frac{1}{\tau_\varphi^{(1,2)}} + \frac{1}{\tau_{12}}.$$

In the high-field limit, $l_B \ll l_\alpha$, the weak-localization corrections to the conductivity have the following asymptoticses

$$\begin{aligned} \Delta\sigma^{(a)} &\approx -\frac{e^2}{\pi^2\hbar} \lambda^{(a)} \sum_{\alpha\beta\gamma} \frac{l_B l_\alpha}{l_\beta l_\gamma} \frac{\tau_\alpha \tau_\beta \tau_\gamma}{\tau_{\alpha\beta} \tau_{\beta\gamma} \tau_{\gamma\alpha}}, \\ \Delta\sigma^{(b)} &\approx \frac{e^2}{\pi^2\hbar} \lambda^{(b)} \sum_{\alpha\beta\gamma} \frac{l_B}{l_\alpha} \frac{\tau_\alpha \tau_\beta \tau_\gamma}{\tau_{\alpha\beta} \tau_{\beta\gamma} \tau_{\gamma\alpha}}, \end{aligned} \quad (33)$$

where the constants $\lambda^{(a)}$ and $\lambda^{(b)}$ are given by

$$\begin{aligned} \lambda^{(a)} &= \sum_{N=0}^{\infty} \left[\int_0^{\infty} dx \exp\left(-\frac{x^2}{2}\right) L_N(x^2) \right]^3 \approx 2.7, \\ \lambda^{(b)} &= \sum_{N=0}^{\infty} \frac{1}{N+1} \left[\int_0^{\infty} dx x \exp\left(-\frac{x^2}{2}\right) L_N^1(x^2) \right]^2 \left[\int_0^{\infty} dx \exp\left(-\frac{x^2}{2}\right) \frac{L_N(x^2) + L_{N+1}(x^2)}{2} \right] \approx 0.94. \end{aligned} \quad (34)$$

III. RESULTS AND DISCUSSION

In this section, we consider the system with two size-quantized levels in detail. To make the consideration closer to experimental applications, each subband will be described with the concentration of carriers $n_\alpha = k_\alpha^2/2\pi$.

In Fig. 2 the solid curves present the dependence of weak-localization correction to the conductivity, $\Delta\sigma$, on magnetic field at various intersubband scattering rates and different level occupations. We assume here that the total relaxation times in the subbands coincide, $\tau_1 = \tau_2$, and the dephasing times are also identical and equal to $10\tau_1$. Fig. 2a shows the case of frequent intersubband transitions, $\tau_{12} \sim \tau_1 \ll \tau_1^\varphi$. Fig. 2b corresponds to relatively rare transitions when the intersubband scattering time is comparable to that of dephasing, $\tau_{12} \sim \tau_1^\varphi \gg \tau_1$. Fig. 2c depicts the case of isolated levels, $\tau_{12} \gg \tau_1, \tau_1^\varphi$.

In the presence of intensive intersubband scattering (Fig. 2a), the magnitude of the weak-localization conductivity correction depends strongly on the excited level occupation in the whole range of magnetic fields. In the opposite case of the relatively weak intersubband scattering, when $\tau_{12} \gg \tau_1$ (Figs. 2b, 2c), $\Delta\sigma$ is practically independent of n_2/n_1 in zero field. The dependence appears in finite fields only, when the magnetic length is comparable with the mean free paths. The reason is the influence of subband concentration on the mean free path which determines the scale of the changing of the weak-localization correction in magnetic field but the value of $\Delta\sigma$ at $B = 0$.

If intersubband scattering is weak enough (Figs. 2b,2c), its role is restricted to additional dephasing. Therefore the difference between the curves presented in Figs. 2b,2c and corresponded to the same ratio n_2/n_1 appears in low fields rather.

The changes of the weak-localization correction in magnetic field, $\Delta\sigma(B) - \Delta\sigma(0)$, calculated in the frame of diffusion approximation with Eq. (32) are presented in Fig. 2 with the dashed curves. This theory is seen to give the reduced absolute value of $\Delta\sigma$ in intermediate fields so that $l_B < \sqrt{l l^\varphi}$ (see Eq. (31)).

The dotted curves in Fig. 2 present the high-field limit ($l_B \ll l_1, l_2$) dependences of

the anomalous magnetoconductivity (33). If the subband concentrations are comparable ($n_2/n_1 = 0.5$ in Fig. 2), $l_1 \sim l_2$, then the weak-localization correction reaches its asymptotic behavior in the range of classically weak magnetic fields. In the opposite case, $l_2 \ll l_1$, the asymptotics of $\Delta\sigma$ corresponding to the excited subband takes place at so high fields that the magnetoconductivity of the ground subband is likely to be of classical nature.

Thus, Fig. 2 shows clearly that the anomalous magnetoconductivity in the whole magnetic field range should be described with the exact expressions (28,29) particularly in the case of relatively small excited subband occupation.

Fig. 3 presents the dependence of the quantum conductivity correction in zero magnetic field, $\Delta\sigma(0)$, on the ratio of the subband concentrations. In the absence of intersubband scattering (solid curve), $\Delta\sigma(0)$ is not affected by the ratio n_2/n_1 because the correction $\Delta\sigma^{(a)}(0) + \Delta\sigma^{(b)}(0)$ of any independent 2D level is universal and equals to $-\frac{e^2}{2\pi^2\hbar} \ln\left(\frac{\tau^\varphi}{2\tau}\right)$. If intersubband transitions take place then $\Delta\sigma(0)$ does depend on n_2/n_1 . However at weak scattering, $\tau_{12} \gg \tau_1$ (dashed curve), the dependence is insignificant. The effect of intersubband scattering is the decreasing of the absolute value, $|\Delta\sigma(0)|$, with respect to the isolated level case. Since weak intersubband scattering acts as an additional dephasing, the effective dephasing time becomes shorter and therefore $|\Delta\sigma(0)|$ decreases. At intensive scattering, $\tau_{12} \sim \tau_1$ (dotted curve), the magnitude of the conductivity correction changes in several times in the shown range of the concentration ratio.

Moreover, one can say that the increasing of the intersubband scattering intensity causes the transition from two-level into one-level system. Indeed, in the absence of intersubband scattering, two independent levels exist. In the case of intensive intersubband scattering, $\tau_{12} \sim \tau_1$, the level division does not take place. There is only one subband effectively with the averaged kinetic parameters. Since the total and dephasing subband times are chosen to be identical respectively, $\tau_1 = \tau_2$, $\tau_1^\varphi = \tau_2^\varphi$, the average parameters of the 'effective subband' coincide with those of separate subbands at the same level occupations, $n_1 = n_2$. The one-level weak-localization correction to conductivity is universal and independent of the level occupation. Therefore at $n_1 = n_2$ the magnitude of $|\Delta\sigma|$ for intensive intersubband

scattering is half as much as for isolated subband system. This difference by a factor of 2 in zero field can be seen in Fig. 3. In the case of the arbitrary level concentration ratio the quantum conductivity correction depends on the intersubband scattering intensity in complicated manner.

Fig. 4 demonstrates the high-field limit asymptotics of the conductivity correction (33), $-\Delta\sigma(B) \times l_1/l_B$, as a function of level occupation ratio. The analysis of Eq. (33) shows the averaging caused by intersubband scattering is complicated and even can change the functional dependence of $\Delta\sigma$ on the level concentrations. It is demonstrated by the curves presented in Fig. 4 and corresponded to different intersubband scattering rates. Specifically, in the absence of intersubband scattering (solid curve) the levels contribute to the conductivity correction independently

$$\Delta\sigma(B) \approx -\frac{e^2}{\pi^2\hbar}(\lambda^{(a)} - \lambda^{(b)}) \left(\frac{l_B}{l_1} + \frac{l_B}{l_2} \right). \quad (35)$$

In the case of very intensive intersubband scattering (dotted curve) the high-field limit expression has the form

$$\Delta\sigma(B) \approx -\frac{e^2}{\pi^2\hbar} \frac{1}{2} \left[\lambda^{(a)} \frac{l_B(l_1 + l_2)^3}{4l_1^2 l_2^2} - \lambda^{(b)} \left(\frac{l_B}{l_1} + \frac{l_B}{l_2} \right) \right]. \quad (36)$$

One can see the quantum corrections obtained with (35) and (36) at the same level concentrations, $n_1 = n_2$, differs by a factor of 2 similarly to the zero field case.

The dependences described in Figs. 2-4 are able to be traced in real quasi-2D structures by variation of the excited subband population as it has been performed in other magnetotransport experiments (see e.g. Ref. 21).

IV. CONCLUSION

The theory of weak localization has been developed for multilevel 2D systems in the whole range of classically weak magnetic fields. Both the diffusion approximation and high-field limit asymptotics have turned out to describe the magnetoconductivity behavior in

very narrow field ranges. For the first time the contribution to the conductivity from all of the self-crossed diagrams has been calculated. It has been shown that the weak-localization correction to conductivity depends strongly on the level concentration ratio and intersubband scattering intensity. Specifically, at the comparable level occupations and the same relaxation times, the conductivity correction of the M -subband system decreases in M times when transiting from the isolated levels to the case of intensive intersubband scattering. The detailed calculations have been performed for the widely investigated system with two occupied size-quantized levels. The results are presented in the form making allowance for comparison with experimental observations.

ACKNOWLEDGEMENTS

This work was supported by the Russian Foundation for Basic Research, projects 00-02-17011 and 00-02-16894, and by the Russian State Programme “Physics of Solid State Nanostructures”.

APPENDIX A:

Let introduce the Fourier-images of the Green functions in zero magnetic field (9)

$$G_{\alpha}^{A,R}(\mathbf{k}) = \frac{1}{\mu_{\alpha} - \hbar^2 k^2 / 2m \pm i\hbar / 2\tau_{\alpha} \pm i\hbar / 2\tau_{\alpha}^{\varphi}}. \quad (\text{A1})$$

From (14) it follows that

$$\mathbf{J}_{\alpha}^{(0)}(\boldsymbol{\rho} - \boldsymbol{\rho}') = \frac{ie\tau_{\alpha}}{m} \sum_{\mathbf{k}} \mathbf{k} \left[G_{\alpha}^R(\mathbf{k}) - G_{\alpha}^A(\mathbf{k}) \right] \exp [i\mathbf{k} \cdot (\boldsymbol{\rho} - \boldsymbol{\rho}')]. \quad (\text{A2})$$

Using Eqs. (10,A1,A2) we obtain the following expression for $\Delta\sigma_2$

$$\Delta\sigma_2 = -\frac{e^2\hbar}{2\pi m^2} \sum_{\alpha\beta\gamma\delta} W_{\alpha\beta\gamma\delta}^2 \tau_{\alpha}\tau_{\beta} \sum_{\mathbf{k}_1\mathbf{k}_2\mathbf{k}_3} \mathbf{k}_1 \cdot \mathbf{k}_2 \left[G_{\alpha}^A(\mathbf{k}_1) - G_{\alpha}^R(\mathbf{k}_1) \right] \left[G_{\beta}^A(\mathbf{k}_2) - G_{\beta}^R(\mathbf{k}_2) \right] \quad (\text{A3})$$

$$\left[G_{\gamma}^A(\mathbf{k}_3)G_{\delta}^R(\mathbf{k}_1 + \mathbf{k}_2 + \mathbf{k}_3) + G_{\gamma}^A(\mathbf{k}_3)G_{\delta}^A(\mathbf{k}_1 + \mathbf{k}_2 + \mathbf{k}_3) + G_{\gamma}^R(\mathbf{k}_3)G_{\delta}^R(\mathbf{k}_1 + \mathbf{k}_2 + \mathbf{k}_3) \right].$$

It is clear this expression could be obtained calculating the diagrams in \mathbf{k} -space from the beginning.

Neglecting the rapidly-oscillating terms $G^A G^A$ and $G^R G^R$, we get

$$\begin{aligned} \Delta\sigma_2 = & -\frac{e^2\hbar}{4\pi m^2} \sum_{\alpha\beta\gamma\delta} W_{\alpha\beta\gamma\delta}^2 \tau_\alpha \tau_\beta \\ & \times \left\{ \sum_{\mathbf{q}\mathbf{k}\mathbf{k}'} \mathbf{k} \cdot (\mathbf{k} - \mathbf{q}) \left[G_\alpha^A(\mathbf{k}) G_\beta^R(\mathbf{q} - \mathbf{k}) + G_\alpha^R(\mathbf{k}) G_\beta^A(\mathbf{q} - \mathbf{k}) \right] G_\gamma^A(\mathbf{k}') G_\delta^R(\mathbf{k}' + \mathbf{q}) \right. \\ & \left. + \sum_{\mathbf{q}\mathbf{k}\mathbf{k}'} \mathbf{k} \cdot \mathbf{k}' \left[G_\alpha^A(\mathbf{k}) G_\gamma^R(\mathbf{q} - \mathbf{k}) G_\beta^A(\mathbf{k}') G_\delta^R(\mathbf{q} - \mathbf{k}') + G_\alpha^R(\mathbf{k}) G_\gamma^A(\mathbf{q} - \mathbf{k}) G_\beta^R(\mathbf{k}') G_\delta^A(\mathbf{q} - \mathbf{k}') \right] \right\}. \end{aligned} \quad (\text{A4})$$

Note that both sums over $\mathbf{q}\mathbf{k}\mathbf{k}'$ converge and, hence, can be calculated separately.

Taking into account that the sums over \mathbf{k} containing the products $G_\alpha^A(\mathbf{k}) G_\beta^R(\mathbf{q} - \mathbf{k})$ are diagonal in subband indices ($\sim \delta_{\alpha\beta}$) due to the conditions (2,3), we obtain

$$\Delta\sigma_2 = -\frac{e^2}{\pi\hbar} \int \frac{d^2q}{(2\pi)^2} \sum_{\alpha\beta} \frac{\tau_\alpha \tau_\beta}{\tau_{\alpha\beta}^2} \left[l_\alpha^2 \tilde{P}_\alpha(q) P_\beta(q) - l_\alpha l_\beta Q_\alpha(q) Q_\beta(q) \right]. \quad (\text{A5})$$

Here

$$\begin{aligned} P_\alpha(q) &= \frac{\hbar}{2\pi N_F \tau_\alpha} \sum_{\mathbf{k}} G_\alpha^A(\mathbf{k}) G_\alpha^R(\mathbf{k} - \mathbf{q}), \\ \tilde{P}_\alpha(q) &= \frac{\hbar}{2\pi N_F \tau_\alpha} \sum_{\mathbf{k}} G_\alpha^A(\mathbf{k}) G_\alpha^R(\mathbf{k} - \mathbf{q}) \left(1 - \frac{\mathbf{q} \cdot \mathbf{k}}{k_\alpha^2} \right), \\ Q_\alpha(q) &= \frac{\hbar}{2\pi N_F \tau_\alpha} \sum_{\mathbf{k}} i \cos(\varphi_{\mathbf{k}} - \varphi_{\mathbf{q}}) G_\alpha^A(\mathbf{k}) G_\alpha^R(\mathbf{k} - \mathbf{q}), \end{aligned} \quad (\text{A6})$$

and $\varphi_{\mathbf{k}}$ is the angular coordinate of the vector \mathbf{k} .

For the case of one occupied subband, the numerical calculation shows that only $q \ll k_F$ give a contribution to the integral in (A5). In this range

$$\tilde{P}(q) \approx P(q) \approx \frac{1}{\sqrt{1 + (ql)^2}}, \quad Q(q) \approx \frac{1 - P(q)}{ql},$$

and integration in (A5) yields

$$\Delta\sigma_2 = -\frac{e^2}{\pi^2 \hbar} \ln 2. \quad (\text{A7})$$

REFERENCES

- ¹ B.L. Altshuler and A.G. Aronov, in *Electron-electron interactions in disordered systems*, edited by A.L. Efros and M. Pollak, (Elsevier, Amsterdam, 1985).
- ² S.V. Kravchenko, W.E. Mason, G.E. Bowker, J.E. Furneaux, V.M. Pudalov, and M. D'Iorio, *Phys. Rev. B* **51**, 7038 (1995).
- ³ J.E. Hansen, R. Taboriski and P.E. Lindelof, *Phys. Rev. B* **47**, 16040 (1993).
- ⁴ N.S. Averkiev, V.A. Berezovets, G.E. Pikus, N.I. Sablina, I.I. Farbstein, *Fiz. Tverd. Tela* **40**, 1554 (1998) [*Phys. Solid State* **40**, 1409 (1998)].
- ⁵ A. Goldenblum, V. Bogatu, T. Stoica, Y. Goldstein and A. Many, *Phys. Rev. B* **60**, 5832 (1999).
- ⁶ G.M. Min'kov, S.A. Negashev, O.E. Rut, A.V. Germanenko, V.V. Valyaev, and V.L. Gurtovoi, *Fiz. Techn. Poluprov.* **32**, 1456 (1998) [*Semiconductors* **32**, 1299 (1998)].
- ⁷ G.M. Minkov, A.V. Germanenko, O.E. Rut, O.I. Khrykin, V.I. Shashkin, V.M. Danil'tsev, *Phys. Rev. B* **62**, 17089 (2000).
- ⁸ N.S. Averkiev, L.E. Golub, S.A. Tarasenko and M. Willander, *Proc. of 25th Int'l. Conf. Phys. Semicond.*, Springer-Verlag (2001), in press.
- ⁹ V.M. Gasparian and A.Yu. Zyuzin, *Fiz. Tverd. Tela* **27**, 1662 (1985) [*Sov. Phys. Solid State* **27**, 1580 (1985)].
- ¹⁰ S. Iwabuchi and Y. Nagaoka, *J. Phys. Soc. Jpn.* **58**, 1325 (1989).
- ¹¹ G. Bergmann, *Phys. Rev. B* **39**, 11280 (1989).
- ¹² N.S. Averkiev, L.E. Golub and G.E. Pikus, *Solid State Commun.* **107**, 757 (1998).
- ¹³ N.S. Averkiev, L.E. Golub and G.E. Pikus, *Fiz. Techn. Poluprov.* **32**, 1219 (1998) [*Semiconductors* **32**, 1087 (1998)].

- ¹⁴ O.E. Raichev and P. Vasilopoulos, *J. Phys.: Condens. Matter* **12**, 589 (2000).
- ¹⁵ M.E. Raikh and T.V. Shahbazyan, *Phys. Rev. B* **49**, 5531 (1994).
- ¹⁶ N.S. Averkiev, L.E. Golub, S.A. Tarasenko and M. Willander, *J. Phys.: Condens. Matter* **13**, 2517 (2001).
- ¹⁷ H. Ebisawa and H. Fukuyama, *J. Phys. Soc. Japan* **53**, 34 (1984).
- ¹⁸ A. Kawabata, *J. Phys. Soc. Japan* **53**, 3540 (1984).
- ¹⁹ A. Cassam-Chenay and B. Shapiro, *J. Phys. I France* **4**, 1527 (1994).
- ²⁰ A.P. Dmitriev, I.V. Gornyi, and V.Yu. Kachorovskii, *Phys. Rev. B* **56**, 9910 (1997).
- ²¹ R. Fletcher, E. Zaremba, M. D'Iorio, C.T. Foxon and J.J. Harris, *Phys. Rev. B* **41**, 10649 (1990).

FIGURES

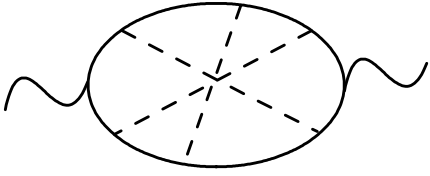
FIG. 1. The diagrams contributing to anomalous magnetoresistance, a) - d), and similar to them, e).

FIG. 2. The dependence of the conductivity correction, $\Delta\sigma$, on magnetic field at various intersubband scattering rates and different level occupations.

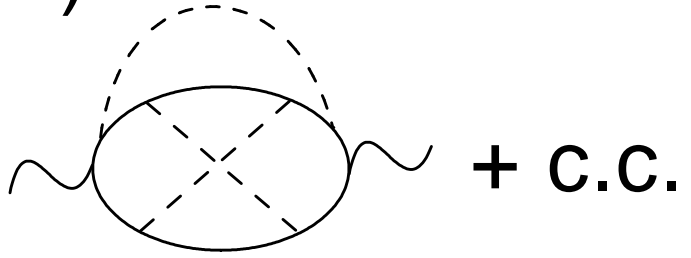
FIG. 3. The dependence of the conductivity correction in zero field, $\Delta\sigma(0)$, on the subband concentration ratio at different intersubband scattering times, $\tau_1/\tau_{12} = 0$ (solid curve), $\tau_1/\tau_{12} = 0.1$ (dashed curve), and $\tau_1/\tau_{12} = 0.5$ (dotted one).

FIG. 4. The dependence of the high-field limit asymptotics of $\Delta\sigma$ on the subband concentration ratio at different intersubband scattering times, $\tau_1/\tau_{12} = 0$ (solid curve), $\tau_1/\tau_{12} = 0.1$ (dashed curve), and $\tau_1/\tau_{12} = 0.5$ (dotted one).

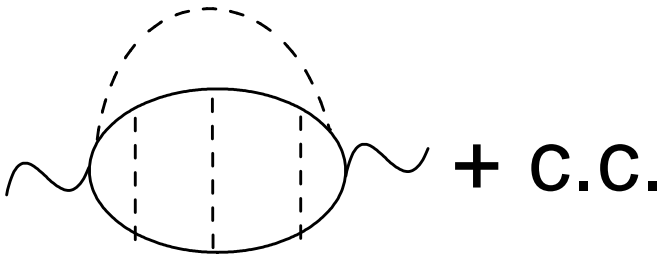
a)



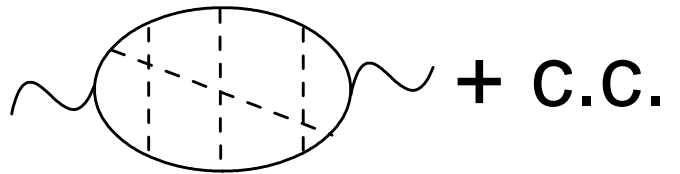
b)



c)



d)



e)

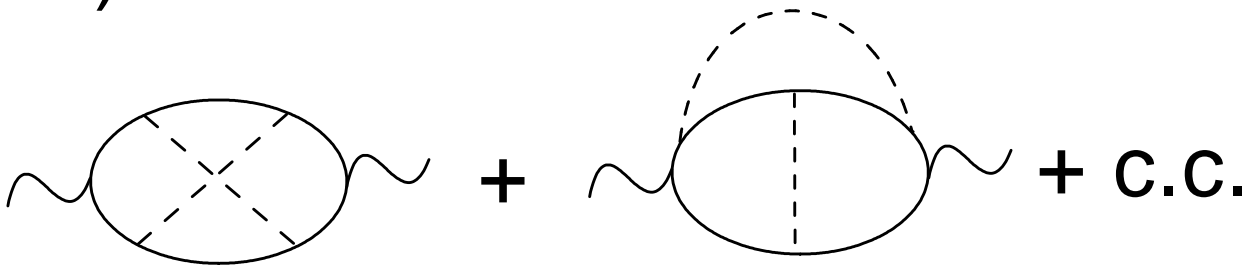


Fig.1 *Averkiev et al.*

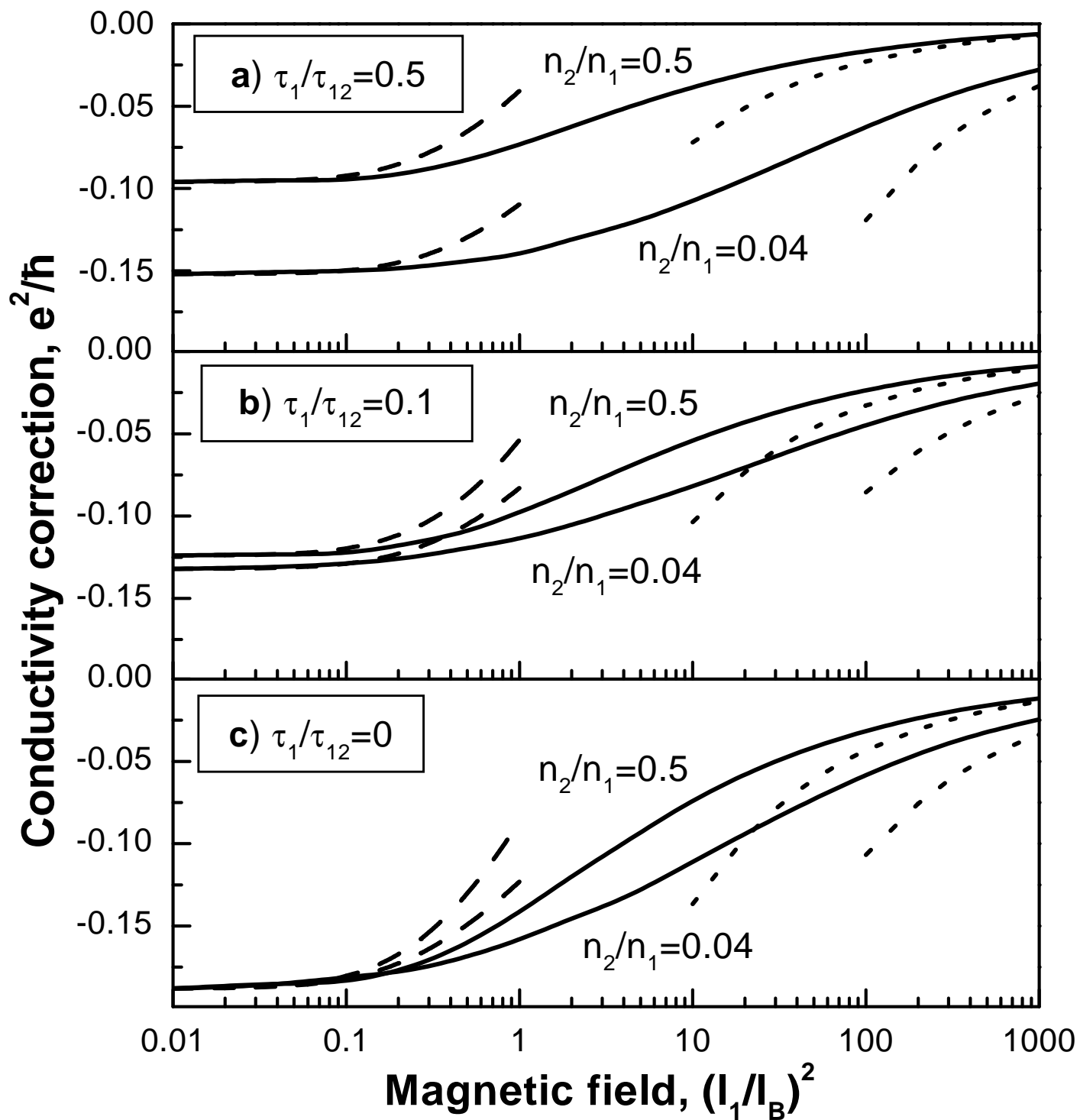


Fig.2 Averkiev et al.

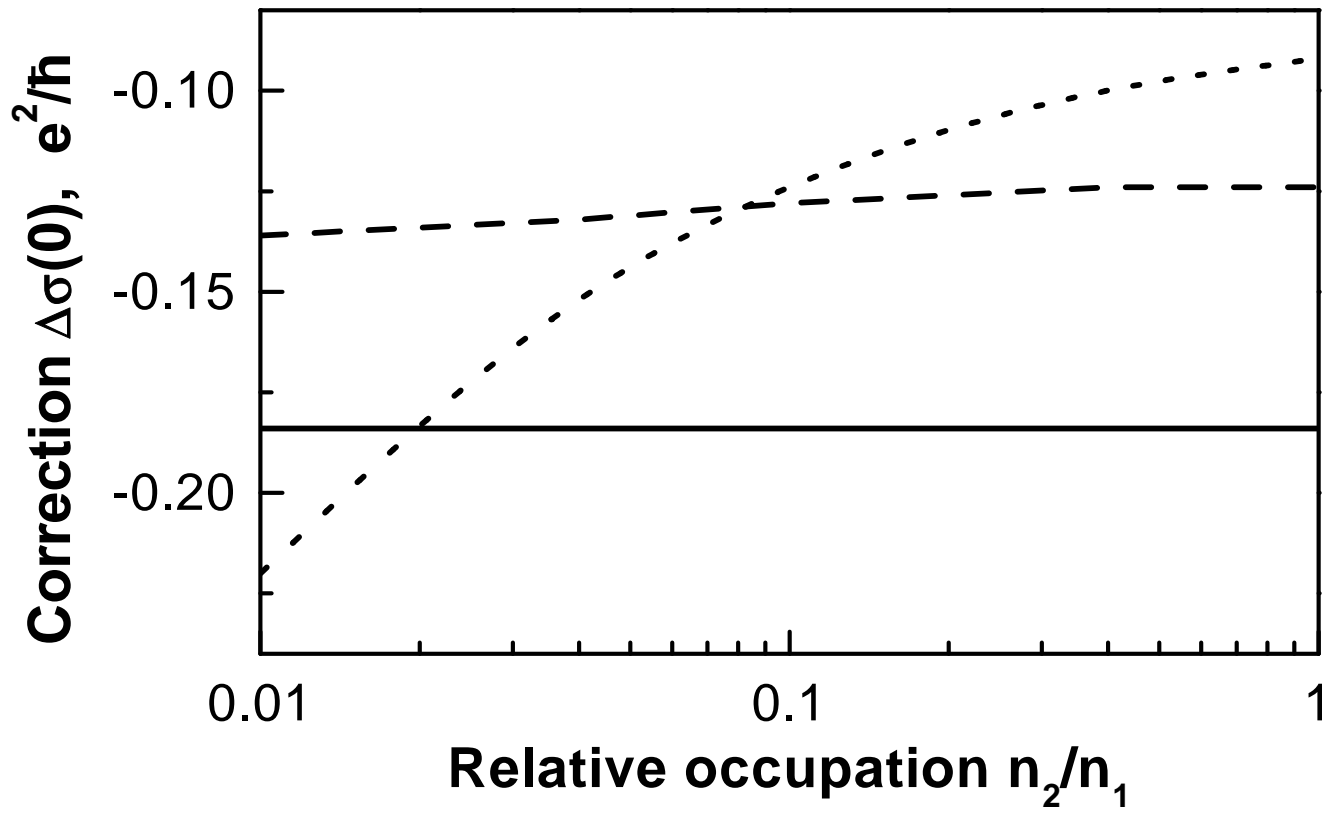


Fig.3 *Averkiev et al.*

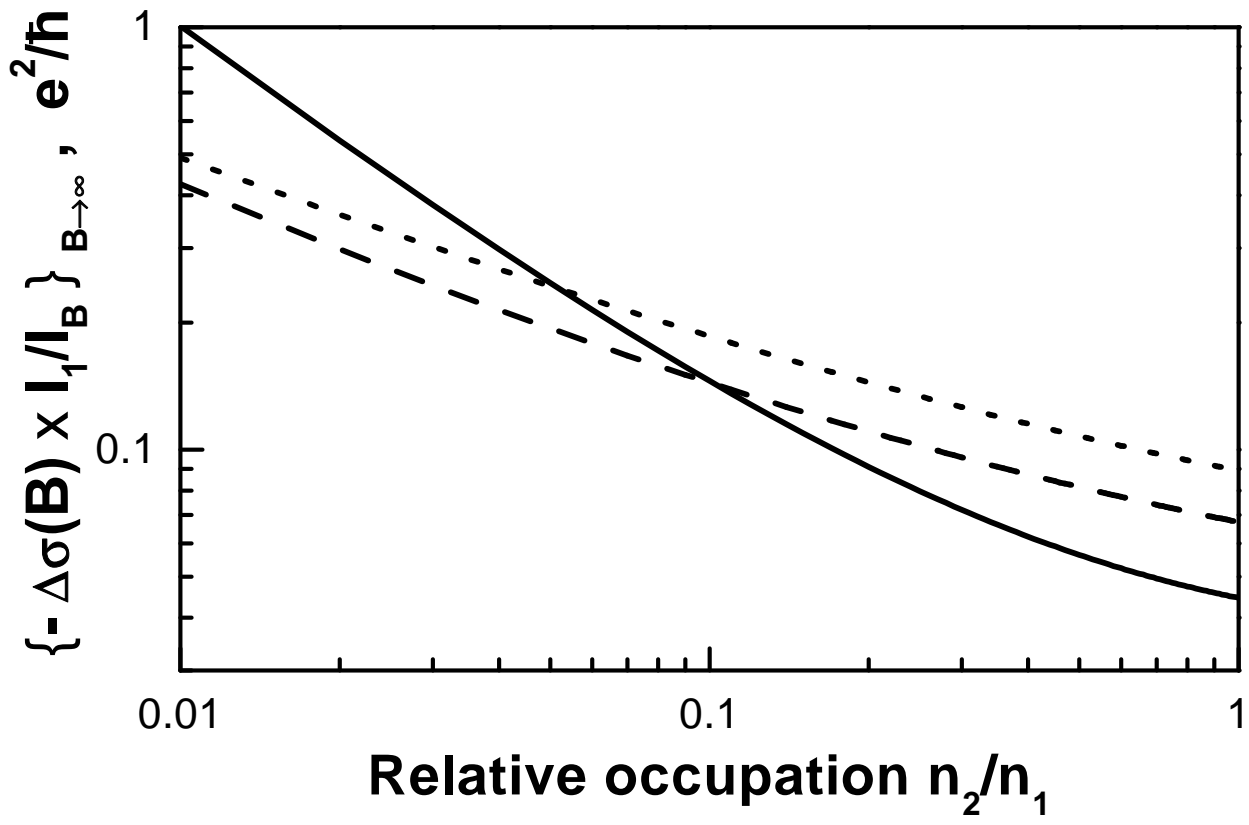


Fig.4 *Averkiev et al.*